Elasticity Measurements Show the Existence of Thin Rigid Cores Inside Mitotic Chromosomes

Bahram Houchmandzadeh* and Stefan Dimitrov‡

*CNRS, Laboratoire Spectromètrie Physique, BP87, 38402 St. Martin d'Hères Cedex, France; and ‡Laboratoire de Biologie Moléculaire et Cellulaire de la Différenciation, INSERM U 309, Institut Albert Bonniot, Domaine de la Merci, 38706 La Tronche, Cedex, France

Abstract. Chromosome condensation is one of the most critical steps during cell division. However, the structure of condensed mitotic chromosomes is poorly understood. In this paper we describe a new approach based on elasticity measurements for studying the structure of in vitro assembled mitotic chromosomes in *Xenopus* egg extract. The approach is based on a unique combination of measurements of both longitudinal deformability and bending rigidity of whole chromosomes. By using specially designed micropipettes, the chromosome force–extension curve was determined. Analysis of the curvature fluctuation spectrum allowed for the measurement of chromosome bending ridigity. The relationship between the values of these two parameters is very specific: the measured chromosome flexibility was found to be 2,000 times lower than the flexibility calculated from the experimentally determined Young modulus. This requires the chromosome structure to be formed of one or a few thin rigid elastic axes surrounded by a soft envelope. The properties of these axes are well-described by models developed for the elasticity of titin-like molecules. Additionally, the deformability of in vitro assembled chromosomes was found to be very similar to that of native somatic chromosomes, thus demonstrating the existence of an essentially identical structure.

Key words: mitotic chromosome structure • elasticity • flexural rigidity • in vitro assembled chromosomes

As eukaryotic cells progress from interphase to mitosis, chromatin undergoes a programmed series of morphological transitions, the most dramatic being its condensation into the familiar metaphase chromosomes. Although mitotic chromosomes have been observed for more than a century, their internal structure is poorly characterized (for review see Earnshaw, 1991). This is due to both the complexity of chromosome structure and technical difficulties related to its investigation. Mitotic chromosomes have been primarily studied by microscopic techniques. However, light microscopy is not well-adapted to the scale of interest (<100 nm); electron microscopy imposes harsh treatment on chromosomes (through the processes of isolation, fixation, and staining) and because of possible artifacts it remains difficult to interpret the results obtained (Hirano and Mitchison, 1993). Cryoelectron microscopy images have been difficult to understand, due to the very low contrast. This relatively poor information has formed the basis of many models, ranging from a hierarchical folding of chromatin (Manuelidis, 1990) to a cross-linked unorganized gel (McDowall et al., 1986) or loops attached to a central scaffold (Paulson and Laemmli, 1977). Different variants of these main models were also suggested in the literature (Rattner, 1992; Saitoh and Laemmli, 1994).

In this paper, we describe the application of a new approach for the investigation of chromosomes, based on their elastic properties. Elasticity reflects the nature and strength of interactions holding materials together, and is strongly dependent on the underlying structure. Elasticity measurements provide hard data from which different models can be confronted. We have measured for the first time the bending rigidity and the force–extension curve of in vitro assembled mitotic chromosomes in *Xenopus* egg extract for the entire range of extensibility. The combination of the data from these two independent measurements gives new critical information on chromosome structure. First, chromosomes display a very specific elastic response: they are 2,000 times more flexible than what could be expected from the measurement of their longitudinal deformability. This strongly suggests the presence of a thin rigid core inside chromosomes, the diameter of which can be estimated, from elasticity calculation, to be

Address correspondence to Bahram Houchmandzadeh, Lab. Spectromètrie Physique, BP87, 38402 St. Martin d'Hères Cedex, France. Tel.: 33-476-514772. Fax: 33-476-514544. E-mail: bahram@spectro.ujf-grenoble.fr

<20 nm. Second, the force–extension measurement of chromosome for high deformations can be well-described by models describing the elasticity of titin-like molecules. Hence, titin-like molecules are good candidates for the rigid inner core.

Materials and Methods

Preparation of Mitotic Extract and Sperm Nuclei

Mitotic *Xenopus* egg extracts were isolated essentially as described by Hirano and Mitchison (1993). In brief, the dejellied eggs were crushed in EB (80 mM β-glycerophosphate, pH 7.3, 15 mM $MgCl_2$, 20 mM EGTA, and 1 mM DTT) supplemented with 10 μg/ml leupeptin and pepstatin, by centrifugation for 20 min at 20,000 *g* in an SW41 rotor (Beckman Instruments). The cytoplasmic fraction was collected and further fractionated by ultracentrifugation at 250,000 *g* for 2 h at 4°C by using the TLS-55 rotor (Beckman Instruments). The lipid layer was sucked very carefully under vacuum, the soluble fraction was removed and recentrifuged for an additional 30 min at 250,000 *g* in order to get rid of the residual membranes. The extract was aliquoted in 25-μl fractions and immediately frozen and stored at −80°C. Demembranated *Xenopus* sperm nuclei were prepared following the procedure of Smythe and Newport (1991) and stored at −80°C. Chromosome were assembled essentially as described by Hirano and Mitchison (1993).

Microscopy and Micromanipulation

Observations were made by an inverted microscope, using 60× phase-contrast objectives (NA = 0.6 or 1.3). Images were acquired through a CCD camera, and recorded on a VCR. When digitized, the resolution of images is 0.21 or 0.4 μm/pixel, depending on the objective used. Two micromanipulators (Sutter MPC-100 and WPI DC30001) were used to direct micropipettes and grab a chromosome by its ends.

Micropipettes were formed to a final inner diameter of 1 μm using a puller (Sutter P-97). To have cylindrical pipette tips, their last 100-μm length was cut by a laboratory-made forge and fire polished.

The deflection of micropipette tips was used to measure forces. A pipette acts like a normal spring, and the force F it applies is proportional to its tip deflection x (for small deflection compared with its length): $F = kx$, where k is the spring constant. The calibration of pipettes was done in two steps. First, a spring of known rigidity (0.84×10^{-2} N/m) was used under the microscope to calibrate an intermediate pipette (rigidity constant 2.4×10^{-3} N/m) which in turn calibrates micropipettes used for elasticity measurements ($2–3 \times 10^{-4}$ N/m). For each pipette, the linearity of the spring was checked over 100 μm deflection, and the error was estimated to be <10%. Deflection of the micropipettes was measured by laboratory-made image correlation techniques and the minimum detectable displacement was ~80 nm.

Elasticity Definitions

Strain and Young Modulus. A thin rod of section S and length L submitted to a force F along its axis would be elongated to $L + \Delta L$. The strain was defined as $\epsilon = \Delta L/L$ and was dimensionless. The Young modulus is the proportionality factor between the force per unit of area and the strain: $F/S = Y\epsilon$. Y has the dimension of a pressure, or energy per unit of volume.

Bending Modulus and the Persistence Length. The energy E needed to bend the thin rod of length L along a circle of radius R reads $E = BL/R^2$. B has the dimension of an energy multiplied by a length.

The resistance to bending of small object like polymers, actin filament, etc., is measured in units of the energy of thermal noise available in the bath, i.e., KT, where K is the Boltzmann constant and T the temperature (at room temperature 300 K, $KT = 4.1 \times 10^{-21}$ J). Thermal noise induces random bending of the object on a scale called the persistence length, $L_p = B/KT$. If the filament is shorter than L_p, it will look like a straight rod (for example, L_p is in the range of few millimeters for microtubules, thus microtubules of 10-μm length seem straight under the microscope). On the other hand, if the filament is much longer than L_p, many random bends could be observed along its length. The measurement of these random bends is a powerful way of measuring the bending rigidity of a filament (Gittes et al., 1993; Ott et al., 1993) without any mechanical manipulation.

Consider tangents at two points belonging to the filaments (see Fig. 2 b). If the points are close to each other (compared with L_p), their tangent will point to nearly the same direction, and the angle θ between them will be close to 0. On the other hand, if the distance between the two points is much higher than L_p, there is no correlation between the tangents, and on average, $<\theta> = \pi/2$. One can show the following relation for the average angle between tangents at two points: $<\cos(\theta(s))> = exp(-s/L_p)$, where s is the arc length between the two points. $<\cos(\theta)>$, which is called the tangent autocorrelation function, means the average of $\cos(\theta)$ over all points along the filament separated by an arc length s. If the filament is confined to two dimensions, $<\cos(\theta)> = exp(-s/2L_p)$ (Doi and Edwards, 1986).

Measurement of the Persistence Length of Chromosomes

The principle of persistence length measurement is the same as described in Ott et al. (1993) for actin filament.

Condensed chromosomes were spread between two coverslips and the reservoir of ~4-μm thickness was sealed. Images of freely fluctuating chromosomes were recorded for few minutes on a tape recorder. A laboratory-developed computer program digitized the images, and a geometrical curve (1 pixel thick) describing the chromosome was obtained by classical skeleton finding algorithms (Chassery and Montanvert, 1991) (this curve is highlighted on chromosome images of Fig. 2 a). Each curve has been reparametrized in order to have constant arc length between consecutive points. The tangent autocorrelation function (see above) has been calculated for each curve and averaged over images of one fluctuating chromosome. The result has been averaged over 16 different chromosomes (~5,000 images have been used for averaging). The process is summarized in Fig. 2, a and b.

Measurement of the Young Modulus

After completion of the chromosome assembly, 5 μl of the solution was deposited in a small reservoir of 20 mm in diameter and 4 mm high, and diluted in 300 μl of EB. A chromosome was grabbed at both ends by two micropipettes. The displacement of one micropipette deformed the chromosome, which in turn applied force to the fixed micropipette. Deflection of the fixed micropipette (which is calibrated at the end of the experiment) measured directly the force applied to the chromosomes (see above). The simultaneous measurement of the length of the chromosome and the deflection of the fixed pipette allowed the determination of the Young modulus (see Fig. 3).

Results

Chromosomes were assembled by incubating demembranated *Xenopus* sperm in mitotic high speed extract isolated from *Xenopus* eggs. The kinetics of chromosome assembly is shown in Fig. 1. As seen, sperm nuclei undergo a series of well-defined structural changes and after 3 h of incubation individual, fully condensed and well-separated chromosomes are formed.

We have performed two independent measurements in order to determine the flexural rigidity and the elongation deformability of these chromosomes (for definitions, see Materials and Methods). The first measurement uses the random bends induced by thermal fluctuations. The second one is performed using two micropipettes, the first to deform the chromosome, and the second to measure the force applied to it. The Young modulus can be deduced when deformations are small. The high deformation regime gives additional critical information on the inner structure of chromosomes.

The in vitro assembled mitotic chromosomes allow for precise measurement of various elastic responses, since they are condensed in cell-free extracts and are easy to manipulate. Their use is critical for the measurement of the flexural rigidity: as they are in a cell-free extract, their

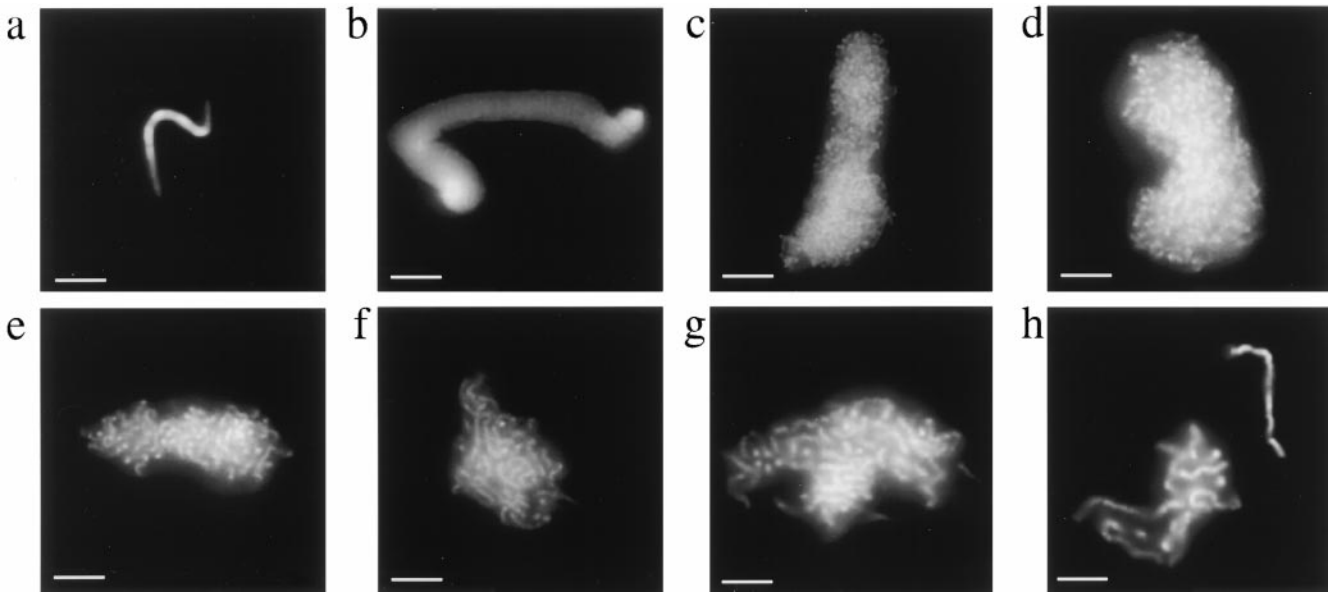

Figure 1. Structural changes of *Xenopus* sperm nuclei in mitotic egg extract; control sperm nuclei (a), decondensed sperm after 10 min of incubation in the extract (b), chromosomal structures (c–g) found after 30, 60, 90, 120, and 150 min, respectively. Upon 180 min of incubation (h) well-separated individual chromosomes were observed. Bars, 5 mm.

random bends are induced by thermal fluctuation. On the other hand, the in vivo chromosomes are constrained by the presence of the cytoskeleton. Moreover, during mitosis, the curvature fluctuations of in vivo chromosomes are due to the nonthermal length fluctuations of microtubules and cannot be assumed to be thermal. Applying force inside the cytoplasm to measure directly the bending modulus presents the same difficulties. All these considerations make the in vitro assembled mitotic chromosomes very suitable for elastic measurements. We will show below that we can reasonably assume the similarity between in vitro and in vivo mitotic chromosomes.

Chromosomes Are Very Flexible Objects

The flexibility of an object is characterized by its bending modulus B. The energy needed to bend the object is proportional to B, and to the square of the induced curvature. We will show below that the measure of this material property shed light on the inner structure of chromosome. This information is also important for a better understanding of the processes taking place at anaphase: during anaphase, sister chromosomes are separated and pulled toward the poles. The force the cell needs to exert in order to pull the chromosome depends on the bending modulus of the chromosomes. If chromosomes can be easily bent, the force which resists their movement (due to the viscosity of the cytoplasm and the constraints imposed by the cytoskeleton network) will be small. On the other hand, if chromosomes are stiff, when pulled toward the poles, they will remain straight and perpendicular to the direction of motion. In this case, pulling them through the cytoskeleton network would need a much higher force.

For elongated objects on the micron and submicron scale, the thermal noise randomly bends the object on a scale called the persistence length L_p, which is proportional to B ($B = KTL_p$, where K is the Boltzmann constant and T is the temperature) (see Materials and Methods). Hence, the analysis of the curvature fluctuation spectrum is a straightforward way of measuring the persistence length.

In brief, in vitro assembled chromosomes were observed under the microscope and their thermal fluctuation was video recorded (Fig. 2 a). Video records of 16 freely fluctuating chromosomes (representing ~5,000 images) were analyzed, and the tangent autocorrelation function was computed. This function shows a perfect exponential decay over approximately one order of magnitude and the deduced chromosome persistence length was found to be 2.7 ± 0.1 μm ($B = 1.2 \times 10^{-26}$ J · m) (Fig. 2 c). Note that this represents only a few times the diameter of the chromosome (0.8 μm) and it is comparable to the persistence length of actin filaments (~10 μm) which are 100 times thinner. The small value of L_p (i.e., high chromosome flexibility) is likely necessary for the achievement of the anaphase.

Chromosomes were visualized by phase-contrast or fluorescent microscopy with Hoechst 258 used for labeling. No difference has been observed due to the presence of the dye at concentrations up to 10^{-6} M. An independent end to end distance measurement of 30 nonlabeled chromosomes gave similar result: $L_p = 3 \pm 0.5$ μm (data not shown).

Chromosome Resistance to Small Elongation

The extensibility of an object upon the action of a force is characterized by its Young modulus Y. The Young modulus depends on the underlying structure of a material. A high Young modulus reflects the fact that a high force is needed to elongate the object. The Young modulus of metals is in the range of 10^{10} to 10^{11} Pa, with those of gels

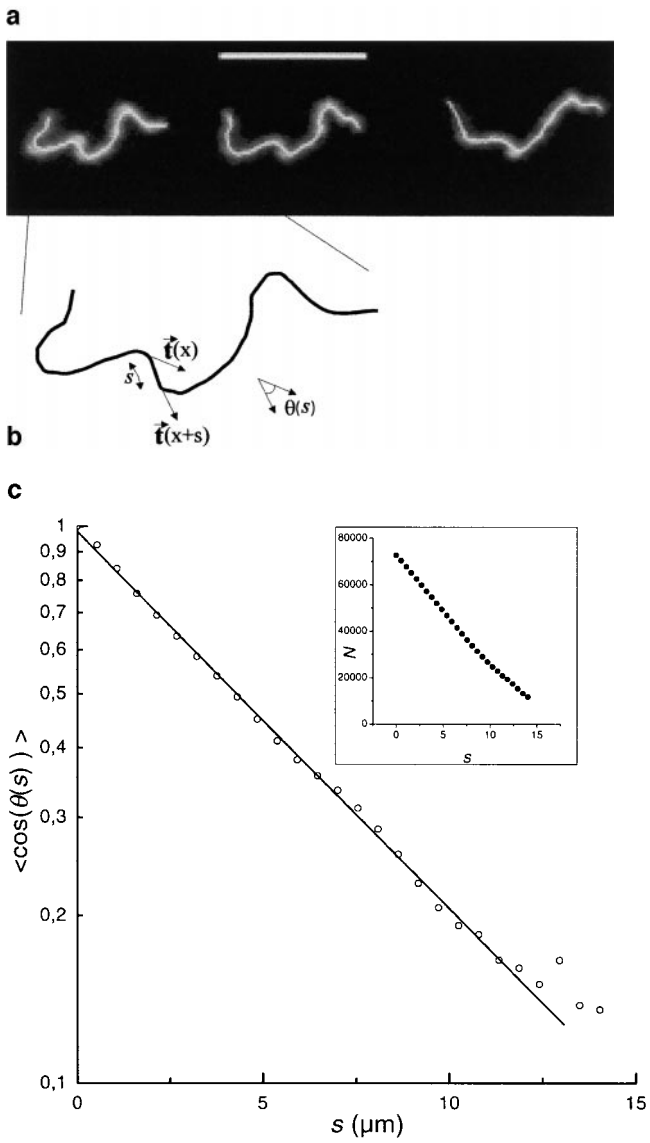

Figure 2. Measurements of chromosome persistence length. In vitro condensed chromosomes were dispersed between two coverglasses and images of freely fluctuating chromosomes were recorded on an S-VHS video recorder. (a) Digitized images of a chromosome, where the computed 1-pixel-thick central skeleton is highlighted (interval between images: 3 s); (b) angle θ (s) between tangents at points separated by an arc of length *s*. (c) The average over 5,000 images of 16 chromosomes of cos(θ(s)) versus *s* curve (tangent autocorrelation function). The curve is fitted by $exp(-s/2L_p)$, where $L_p = 2.7 \pm 0.1$ μm. Chromosomes were visualized by phase-contrast or fluorescent microscopy with Hoechst 258 used for labeling. (Inset) Number of samples used to perform the average, as a function of arc length.

lays in the 10^6 to 10^7 Pa interval. Microtubules and actin filaments have a Young modulus of 10^9 Pa. During mitosis, chromosomes are submitted to elongation stress due to microtubules and motors. A careful measurement of chromosome elongation at different times and the knowledge of their Young modulus should allow the determination of the force exerted on them at different stages of mitosis, a subject still submitted to debate after the article published by Nicklas (1983).

In this work, we have measured the chromosome Young modulus, and we will discuss below the relevance of this elastic constant for the chromosome underlying structure.

For a thin rod of section S and length L submitted to a force F along its axis, the Young modulus is defined as: $Y = F/S(\Delta L/L)^{-1}$, where ΔL is the elongation induced by the force (see Materials and Methods). We determined the chromosome Young modulus from its force–extension curve by using the micropipette technique. A chromosome was suspended between two micropipettes, using a small amount of aspiration. The chromosome was then stretched by moving one of the micropipettes at a constant speed, while the length of the chromosome and the deflection of the other micropipette (used as a nanodynanometer) were simultaneously measured after recording the images on a video recorder (Fig. 3). For a small deformation ($\Delta L/L <$ 1) and stretching rate (<1 μm/s), the curve of force versus deformation is reversible over many cycles. Fig. 4 shows a typical measurement for two different chromosomes. The Young modulus of chromosomes (measurements performed on 11 different chromosomes) is found to be in the 800–1,350 Pa range, with an average value of 1,100 Pa.

Chromosomes Are Highly Extensible Objects

Chromosomes can be elongated manifolds. For higher deformations, hysteresis is observed (Fig. 5). The elasticity ceases to be linear and the behavior is similar to that observed for long biological polymers such as titin and tenascin (Kellermayer et al., 1997; Rief et al., 1997; Tskhovrebova et al., 1997; Oberhauser et al., 1998). Successive deformation cycles, where the final extension is gradually elevated, induce also an irreversible transition in chromosome structure: after each cycle, the chromosome is softened and the next stretch necessitates a lower force in order to reach the same elongation. The maximum length to which chromosomes can be extended is variable: disruption of different chromosomes is observed for elongation between 12 and 100 times their original length. The force–extension curve of chromosomes that did not break after being stretched ~15 times their original length show a plateau ~5–10 nN (Fig. 6 a). This plateau is associated with the partial unraveling of the chromosomes: chromosome parts exhibiting similar diameter as the nondeformed ones are found separated from each other and are connected by thin filaments.

The thin filaments are not observable under the microscope, but their presence can be demonstrated upon moving the micropipette which induces displacement of the whole structure (Fig. 6 b).

Measurement of the Elastic Constants of Demembranated Sperm Nuclei

Chromosomes were assembled from *Xenopus* sperm nuclei. Since these structures showed unusual elastic properties, we have been further interested to understand whether this behavior was specific to mitotic chromosomes only, or if it could be observed also on the "parental" structure, i.e., the sperm nucleus.

In contrast to mitotic chromosomes, demembranated sperm nuclei appear as very rigid objects for both flexural and longitudinal stress. The Young modulus Y of sperm

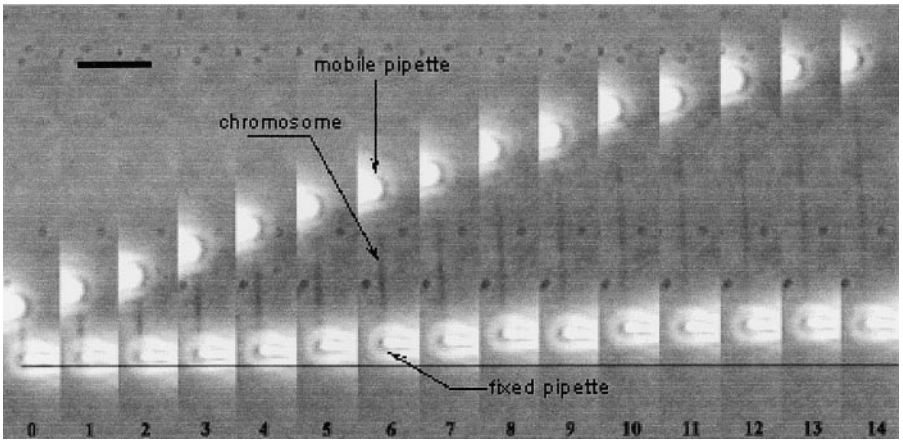

Figure 3. Successive micrographs of typical force–extension measurement. A chromosome was suspended between two micropipettes and stretched with the upper one. The lower micropipette (prepared in order to have $K \approx 2$–4×10^{-4} N/m spring constant) was calibrated after each measurement. The length of the chromosome and the force applied to it were measured after digitization of the recorded images. Bar, 10 μm.

nuclei has been measured by the same micropipette technique as described above. The value of Y, measured on 11 different sperm nuclei, was found to be 200 ± 50 kPa. Note that this value is two orders of magnitude higher than those of mitotic chromosomes.

The bending rigidity B of the sperm nucleus is too high to allow measurable thermal fluctuations. Thus, we used the micropipette directly to induce bending of sperms, and measured the force–curvature relation. The value of the bending rigidity obtained from three different samples was found to be $1 \pm 0.5 \times 10^{-20}$ J · m, which corresponds to a persistence length of 2.5 m! This is six orders of magnitude higher than for mitotic chromosome.

Discussion

In this work we have studied the elastic behavior of in vitro assembled chromosomes in *Xenopus* egg extracts. Let us summarize the results obtained: we have measured a chromosome Young modulus of 1,100 Pa, and a persistence length of 2.7 μm. The relations between these values and the nonlinear high deformation behavior have profound consequences on the underlying chromosome structure and lead us to propose a model for the inner organization of mitotic chromosomes.

Below, we will first discuss the fact that in vitro assembled chromosomes have similar substructures as their so-

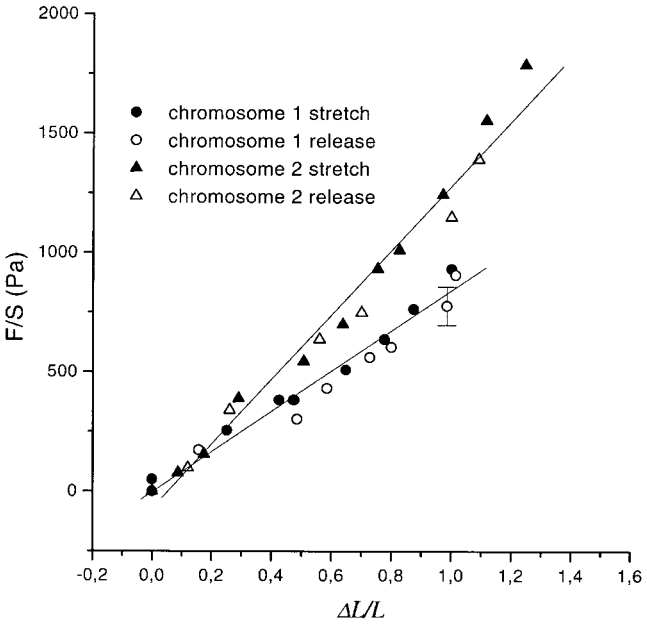

Figure 4. The force per section versus deformation curve for two different chromosomes. $Y_1 = 840$; $Y_2 = 1{,}350$. For simplicity, the error bar for one point only is shown. Chromosome diameter is 0.8 μm (section 0.5 μm^2). The initial length of chromosome 1 was 9.5 μm, and that of chromosome 2 was 8.7 μm.

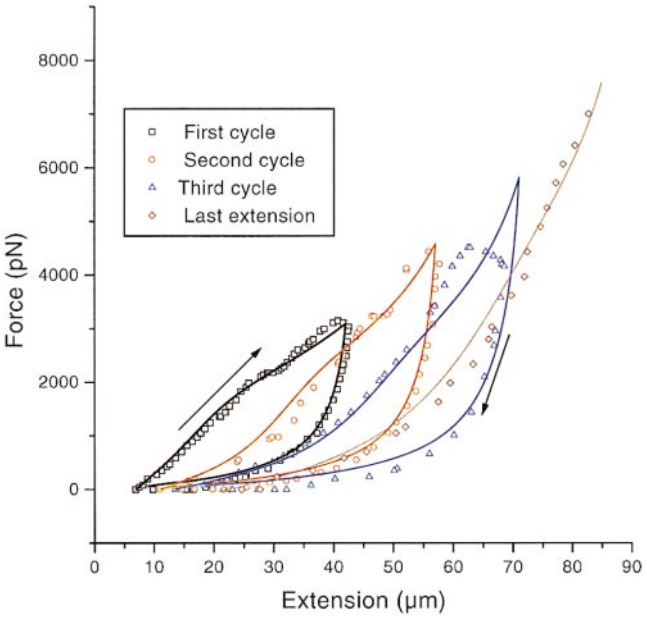

Figure 5. Force–extension cycles of a single chromosome (initial length 7 μm) for high deformations at 1 μm/s. The solid lines represent the numerical resolution of equations of 45 parallel titin-like molecules. 25% of the domains are supposed to be irreversibly unfolded after the first cycle, 40% after the second one, and 60% after the third one. The parameters used to solve the kinetic equations were: $l_{unfold} = 29$ nm, $l_{fold} = 4$ nm, $A = 2$ nm, $E_a = 22$ pN nm, $\Delta x = 0.1$ nm, $\Delta x' = 2$ nm, $\omega_0 = 1\ s^{-1}$. The initial chain deformation, due to chromatin pressure, is taken as $z/L = 0.5$.

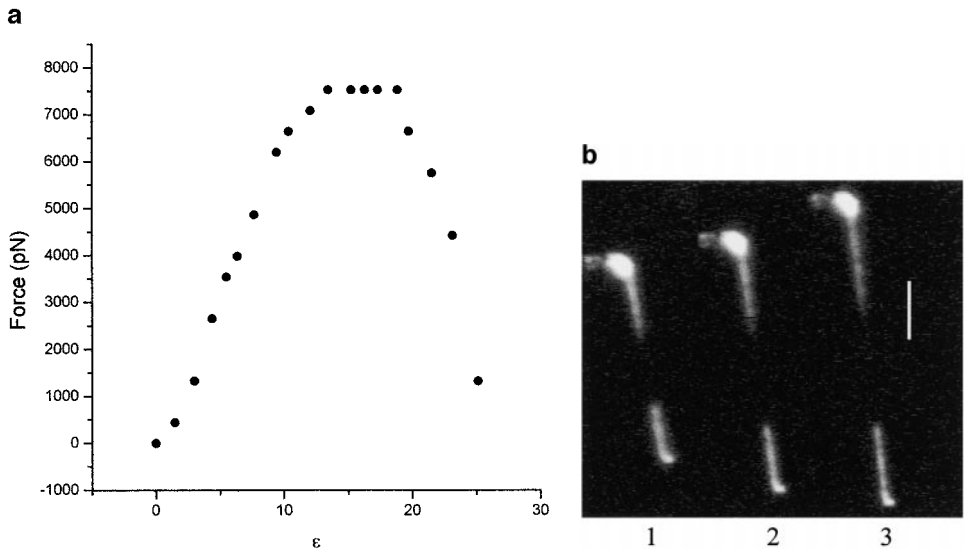

Figure 6. (a) Apparition of plateau regime before the breakdown of the chromosome for high extension regime (initial chromosome length: 7.8 μm). (b) If the extension is stopped at the middle of the plateau regime, domains of thick chromosome connected by thin filaments are observed. Three successive micrographs of a partially unraveled chromosome are shown, where one micropipette moves to show the existence of the connecting thin filament.

matic counterparts. Next, we will show that our data strongly suggest the existence of thin rigid chromosome axes essential for mitotic chromosome organization. Finally, we will demonstrate that the nonlinear force–extension relationship observed for high deformations requires these rigid axes to be built similarly to an ensemble of highly elastic proteins.

Comparison of In Vitro Assembled and Somatic Chromosomes

An important question to be addressed regarding the data presented is to what extent in vitro assembled chromosomes are related to the in vivo ones. Both types of chromosomes possess a similar overall shape and size as well as biochemical compositions (Hirano and Mitchison, 1993). But their internal structures are not really known and the subject is still controversial (Hirano and Mitchison, 1993; Poljak and Käs, 1995). Determination of their material properties is well-adapted to answer this question. The Young modulus of chromosomes for small deformations has been measured by Nicklas (1983) for grasshopper anaphase chromosomes (500 Pa) and by Houchmandzadeh et al. (1997) for metaphase newt lung chromosomes (1,000 Pa). Moreover, the last authors showed that chromosomes can be stretched up to 100 times their initial length, and if the deformation is less than 10, their original length can be restored. Compared with these results, in vitro assembled *Xenopus* chromosomes are very similar: their Young modulus is within the same range as somatic ones (1,100 Pa), their original length can be restored for 5–10 times deformations, and they can be plastically deformed up to 100 times. All these similarities lead us to conclude that the internal structures of both assembled in vivo and *Xenopus* egg extract chromosomes are essentially identical.

Chromosomes Are Formed of Thin Rigid Axes, Surrounded by a Soft Envelope

Let us summarize the results presented in the previous sections: the persistence length L_p (which characterizes the resistance to bending) of chromosomes is 2.7 μm, while their Young's modulus Y (which is a measure of their resistance to stretching) is of the order of 1,000 Pa. No information about the underlying structure can be obtained from each value taken independently, but their relation has profound consequences. For a large class of material organizations, the relation between L_p and Y obeys the following relation (Landau and Lifshitz, 1986; Love, 1992):

$$L_p = CYr^4/KT \quad (1)$$

where r is the radius of the object, C a numerical constant of order of unity ($\pi/4$ for a solid cylinder), T the absolute temperature, and K the Boltzmann factor. This relation is due to the fact that bending (with elastic response proportional to L_p) induces elongation/compression above/below a central neutral plane, with an elastic response that is proportional to Y. Eq. 1 would hold, for example, if the chromosome were formed of a crystalline polymer, if it were a gel-like material (the chromatin fiber cross-linked to itself by some molecular agent at random intervals), or, most importantly, if it were formed of a thinner fiber which folded helically to make the whole chromosome. Examples of biological objects obeying Eq. 1 are microtubules and actin filaments (Gittes et al., 1993). In fact, Eq. 1 does not hold for the chromosome: as the radius of the chromosome is 0.4 μm, the right hand of Eq. 1 equals ~5 mm, which is 2,000 times higher than the measured value of the persistence length. Roughly speaking, chromosomes appear to be hard when stretched, but very soft when bent.

To explain our results, one has to imagine a model of chromosome organization in which the two apparent modes of elasticity (bending and stretching of the whole structure) are not related by Eq. 1. A straightforward explanation is to suppose that the chromosome is formed of a thin rigid (and elastic) core, surrounded by a soft envelope. As the core is thin and the persistence length varies as the fourth power of the radius, the whole object can be

bent easily, while its stretching implies large forces. As a commonplace example, this is similar to the case of electric wires, which can be bent easily because they are formed of many thin filaments of copper, but cannot be elongated.

In such a model, chromosomes would possess a core with a Young's modulus higher than 10^6 Pa and a diameter $<$20 nm, while the Young's modulus of the surrounding soft envelope would be $<$1 Pa. In the limit case where the diameter of the core is 20 nm, the resistance to bending and stretching of the whole chromosome is ensured only by the thin axis and there is no contribution from the soft envelope.

If, on the other hand, the diameter of the axis is much $<$20 nm, the resistance to bending of the thin axis becomes negligible: the persistence length of the whole chromosome is due only to the soft envelope, while its resistance to stretching is due only to the thin axis. In this latter case, bending and stretching of the whole chromosome involve independent elastic elements (see Appendix) and each elastic element can be treated separately. Moreover, if we suppose that the diameter of the axis lies in the molecular range (and has negligible persistence length), one does not even need to assume that the core itself obeys classical elasticity, the only important attribute of the core being its resistance to elongation. This resistance, for the whole range of extension, can be computed using classical polymer theory, as for proteins such as titin and tenascin (Kellermayer et al., 1997; Oberhauser et al., 1998).

Both of the above limit cases can consistently explain the relation between the measured values of the elastic constants of chromosomes. We will show below that deforming chromosomes by a large amount favors the second hypothesis.

For simplicity in our calculations we have considered only one rigid axis. However, one can envisage several such axes distributed through the whole section of the chromosome, connected to each other by the soft envelope and constituting a columnar phase. From the measurement of L_p and Y it is not possible to estimate the number and the space distribution of these axes. However, by using the same calculation, one can prove that the thickness of each axis should be $<$20 nm, and that their Young's modulus should be of the order of Y_{in}/N, where N is the number of axes and Y_{in} the Young's modulus of the inner structure for the one-axis case.

Before going further, note that Eq. 1 holds for the sperm nucleus, the other very compact organization of DNA we have measured. Thus, sperm nuclei should have a homogeneous or helical substructure. The remodeling of the very condensed sperm nucleus in the *Xenopus* extract is associated with the removal of the protamine-like proteins and the uptake of numerous histone and nonhistone proteins (Dimitrov et al., 1994; Hirano, 1995). Our data show that these changes in protein composition result in dramatic changes in the underlying structure.

Structure of the Chromosome Axes

How are the rigid axes built? As shown above (Fig. 5), chromosomes can be stretched by many times their length; therefore, the axes store a large reservoir of length. Moreover, the chromosome force–extension curve shows a strong hysteresis and a gradual softening. Recently, similar force–extension behavior has been reported for a class of proteins that include titin and tenascin (Kellermayer et al., 1997; Rief et al., 1997; Tskhovrebova et al., 1997; Oberhauser et al., 1998), and the presence of titin inside mitotic chromosomes has also been demonstrated (Machado et al., 1998).

Native titin is a long (1 μm) polymer, formed of ~250 Ig domains. Each domain, in its native form, has a length of ~4 nm. Upon stretching, each domain can unfold and reach an overall length of ~30 nm. When submitted to a gradually increasing force, the titin molecule first straightens from a coiled form, and when the force reaches a critical value, domains begin to unfold gradually. The elasticity of titin (and tenascin) is well-described by a modified worm-like chain model (Kellermayer et al., 1997; Rief et al., 1997; Tskhovrebova et al., 1997).

The solid lines of Fig. 5 represent numerical resolution of several cycles of chromosome elongation, assuming 45 titin-like molecules per chromosome. The equation describing the force–elongation relation of these polymers is detailed in Kellermayer et al. (1997) and Rief et al. (1997). Note that the persistence length of each titin molecule in this model is 2 nm. The total contribution of titin-like axes to the persistence length of the whole chromosome is $<$100 nm. Thus, the persistence length of the chromosome (3 μm) is mostly due to the chromatin matrix. The chromatin matrix itself does not contribute to the resistance to elongation. This model belongs to the limit case discussed above, where the resistance to bending and stretching of the whole chromosome is supposed to be due to independent elastic substructures.

To explain the softening of the chromosome after a deformation cycle, we have assumed that, after each cycle, a fraction of unfolded domains fails to refold. Similar behavior has been observed for the elasticity of titin (Kellermayer et al., 1997). As seen, the model is in impressive agreement with our experimental data and this implies that the rigid axes are built like titin molecules. Thus, proteins or protein complexes possessing titin-like elastic properties should be the main components of the chromosome axes. What are these proteins? At present we are not in a position to give a definite answer. Obviously, a good candidate may be titin itself, since it has been found to be associated with mitotic chromosomes (Machado et al., 1998). Other plausible candidates are the proteins from the SMC family (Hirano et al., 1995). These proteins exist in *Xenopus* egg extract as high molecular complexes called condensins (Kimura et al., 1998). Condensin immunodepleted extract is no longer able to assemble chromosomes, and thus condensins are essential for chromosome condensation and architecture (Strunnikov, 1998). In addition, it was shown that bacterial SMC proteins have their coiled-coil domains organized around a hinge (Melby et al., 1998), which seems to be structurally flexible. Since the SMC proteins are very conservative, condesins could conceivably exhibit similar hinge structure. If this is really the case, the chromosome resistance to elongation will be determined by the elastic properties of the hinge. Recently, a model for chromosome condensation based on the "scis-

soring" action of the SMC proteins was proposed by Hirano (1999).

The presence of a single backbone of nonhistone proteins (a scaffold), responsible for the organization of metaphase chromosomes, has been postulated in the past (Paulson and Laemmli, 1977). However, the existence of the scaffold structure in intact mitotic chromosomes has remained controversial (Earnshaw, 1991). Indeed, the scaffold was observed only upon treatment of mitotic chromosomes with different detergents and salts and thus it was not clear whether the observed structure was not an artifact due to the precipitation of high molecular weight chromosomal proteins (Okada and Comings, 1980; Hirano and Mitchison, 1993). For example, the first biochemically defined component of the scaffold was topo II, but depletion of topo II from in vitro assembled chromosomes (using salt extraction, as in Hirano and Mitchison, 1993) did not change their elastic properties (data not shown). Additionally, within the most sophisticated version of this model, the scaffold and the chromatin loops form an ~200-nm fiber (Rattner, 1992; Saitoh and Laemmli, 1994), which further folds helically to assemble the mitotic chromosome. However, such a structure is not compatible with the measured chromosome elasticity: for this model, the diameter of the object (the outer diameter of the supposed helix) which ensures the elastic responses is of the order of the chromosome thickness. Hence, if the measured Young modulus is 1,000 Pa, the persistence length would be in the millimeter range, three orders of magnitude larger than the measured value. The same argument can be made for other model of chromosome structure (homogeneous gel-like; McDowall et al., 1986), hierarchical helical folding (Sedat and Manuelidis, 1978; Manuelidis, 1990), which cannot explain the apparent discrepancy between the measured values of chromosome elasticity.

In our previous work on in vivo chromosomes (Houchmandzadeh et al., 1997), based on a limited amount of information, we had favored a model of chromosome organization based on helical folding of a thin filament. The diameter of the thin filament was supposed to be four times smaller than that of the mitotic chromosome. The argument was based on the huge extensibility of chromosomes, on the knowledge of their Young's modulus, and on geometrical considerations. Two critical data were missing at that time: the value of the persistence length of chromosomes and the force–elongation relation for high chromosome deformation, which are, as stressed above, very difficult to measure in vivo. These data have been obtained in this work, and as shown above, are not compatible with the model of helical organization.

In conclusion, we have developed a novel approach for studying chromosome structure. Our experiments show that mitotic chromosomes exhibit specific elastic responses. Therefore, we propose a model for chromosome structure based on a single or several thin elastic axes surrounded by a soft envelope (Fig. 7). The axes are proposed to consist of elastic titin-like molecules, while the envelope contains chromatin. The chromatin material is attached to the axes and is responsible for keeping the axes close together. The resistance of mitotic chromosomes to bending is ensured by the chromatin matrix, where the axes are responsible for the resistance of chromosome to elongation.

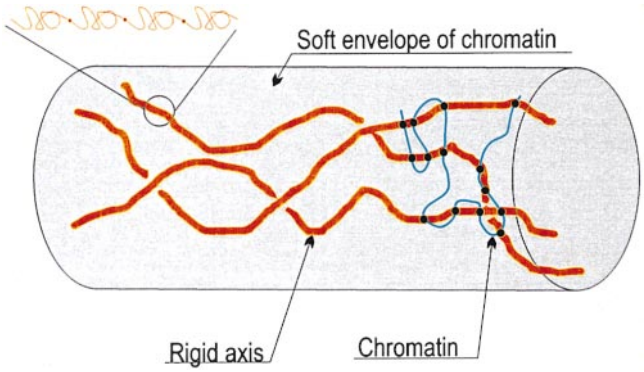

Figure 7. Schematic representation of mitotic chromosome structure based on elastic measurements. The chromosome is proposed to be formed of a few rigid axes, surrounded by a soft envelope of chromatin attached to the axes. The rigid axes are built of titin-like molecules, formed of repetitive domains, which can be unfolded upon application of force.

The condensation state of the chromosome is determined by the interplay between the entropic forces exerted by the axes which tend to collapse them into a random coil and the excluded volume effects due to chromatin (Marko and Siggia, 1997). Moreover, local decondensation of chromosomes can be achieved by a simple unfolding of axis protein domains.

Appendix

As noted above, many material organizations obey the relation:

$$B = CYr^4 \tag{2}$$

where B is the bending modulus of the object, Y its Young modulus, r the radius, and C a numerical constant of order of unity. The persistence length L_p of the chromosome is B/KT.

Mitotic chromosomes do not obey this relation. As the bending modulus varies as the fourth power of the diameter, a straightforward explanation is to suppose that the diameter of the object which ensures the resistance to stretching is much smaller than the apparent diameter of the chromosome, and its Young modulus much higher. We can estimate the order of magnitude of such an object. Suppose for simplicity that the chromosome is formed of one rigid axis of radius r_{in} and Young modulus Y_{in}, surrounded by a soft envelope of radius r (the radius of the whole chromosome) and Young modulus Y_{out}. The measured values of elastic constants of the whole chromosome are related to the elastic constants of these two substructures through:

$$Y = Y_{out} + (Y_{in} - Y_{out})\gamma^2 \tag{3}$$

$$4B/\pi r^4 = Y_{out} + (Y_{in} - Y_{out})\gamma^4 \tag{4}$$

where $\gamma = r_{in}/r$. We will note below $Y^* = 4B/\pi r^4$. For in vitro assembled chromosomes, $r = 0.4$ μm, $Y = 1{,}000$ Pa, and $Y^* = 0.6$ Pa. Note that there are three variables (r_{in}, Y_{in}, Y_{out}) and only two equations, so exact values for the

variables cannot be obtained. However, an upper bound for γ is easily found from Eq. 3 and Eq. 4:

$$Y\gamma^2 - Y^* = Y_{out}(\gamma^2 - 1) \leq 0 \quad (5)$$

as $\gamma < 1$, and thus

$$\gamma \leq \sqrt{Y^*/Y} = 0.025 = \gamma_{max} \quad (6)$$

which implies

$$r_{in} \leq r\sqrt{Y^*/Y} = 10\ \text{nm} = r_{max} \quad (7)$$

where r_{max} is the maximum radius of the elastic axis. As $\gamma \ll 1$ and $Y^* \ll Y$, the elastic constant of the two substructures are: $Y_{in} \approx Y/\gamma^2$ and $Y_{out} \approx Y^* - Y\gamma^2$.

There are two interesting limit cases. First, if $r_{in} \approx r_{max}$, $Y_{out} \approx 0$ and $Y_{in} \approx 1.5 \times 10^6$ Pa. In this case, the soft envelope does not contribute to resistance to stretching, nor to resistance to bending and the elasticity of the whole chromosome reduces to the elasticity of the thin axis. The other limit case is when $r_{in} \ll r_{max}$, the resistance to bending of the thin axis becomes negligible, and the persistence length of the chromosome is only due to the soft envelope of chromatin ($Y_{out} \approx 0.6$ Pa). The contribution to stretching on the other hand is only due to the rigid axis. In this case, bending and stretching involve independent elastic elements. Note that if we suppose the radius of the axis to be much <10 nm, it becomes difficult to suppose that it still obeys classical elastic theory. The axis will still resist stretching like classical polymers or titin-like molecule. As the bending and the stretching of the whole chromosome are uncoupled, one can treat each substructure independently: the resistance to stretching through the modified worm-like chain model (as for titin; Kellermayer et al., 1997) for the thin axis, and the resistance to bending using elasticity for the soft envelope (a theoretical ground for this calculation is proposed by Marko and Siggia, 1997).

We thank D. Dimitrov, J. Hayes, M. Vallade, B. Berge, E. Katz, and M. Creaven for fruitful discussions and careful reading of the manuscript. We also thank A. Libchaber and J.-J. Lawrence for support throughout the course of this work.

This research was supported by the Centre National de Recherche Scientifique.

Received for publication 24 November 1998 and in revised form 23 February 1999.

References

Chassery, J., and A. Montanvert. 1991. Geometrie Discrete en Analyse d'Image. Hermes, Paris.

Dimitrov, S., M.C. Dasso, and A.P. Wolffe. 1994. Remodeling sperm chromatin in *Xenopus laevis* egg extracts. *J. Cell Biol.* 126:591–601.

Doi, M., and S.F. Edwards. 1986. The Theory of Polymer Dynamics. Oxford University Press, Oxford.

Earnshaw, W.C. 1991. Large scale chromosome structure and organization. *Curr. Opin. Struct. Biol.* 1:237–244.

Gittes, F., B. Mickey, J. Nettleton, and J. Howard. 1993. Flexural rigidity of microtubules and actin filaments measured from thermal fluctuations in shape. *J. Cell Biol.* 120:923–934.

Hirano, T. 1995. Biochemical and genetic dissection of mitotic chromosome condensation. *Trends Biochem. Sci.* 20:357–361.

Hirano, T. 1999. SMC-mediated chromosome mechanics: a conserved scheme from bacteria to vertebrates. *Genes Dev.* 13:11–19.

Hirano, T., and T.J. Mitchison. 1993. Topo II does not play a scaffolding role in the organization of mitotic chromosomes assembled in *Xenopus* egg extract. *J. Cell Biol.* 120:601–612.

Hirano, T., T.J. Mitchison, and J.R. Sweldow. 1995. The SMC family: from chromosome condensation to dosage compensation. *Curr. Biol.* 7:329–336.

Houchmandzadeh, B., J.F. Marko, D. Chatenay, and A. Libchaber. 1997. Elasticity and structure of eukaryote chromosomes. *J. Cell Biol.* 138:1–12.

Kellermayer, M.S.Z., S.B. Smith, H.L. Granzier, and C. Bustamente. 1997. Folding-unfolding transition in single titin molecules. *Science.* 276:1112–1116.

Kimura, K., M. Hirano, R. Kobayashi, and T. Hirano. 1998. Phosphorylation and activation of 13S condensin by cdc2 in vitro. *Science.* 282:487–490.

Landau, L.D., and E.M. Lifshitz. 1986. Theory of Elasticity. Pergamon Press, Tarrytown, NY.

Love, A.E.H. 1992. A Treatise on the Mathematical Theory of Elasticity. Dover, New York.

Machado, C., C.E. Sunkel, and D.J. Andrew. 1998. Human antibodies reveal titin as a chromosomal protein. *J. Cell Biol.* 141:321–333.

Manuelidis, L. 1990. A view of interphase chromosome. *Science.* 250:1533–1540.

Marko, J.F., and E. Siggia. 1997. Polymer model of meitotic and mitotic chromosomes. *Mol. Biol. Cell.* 8:2217–2231.

McDowall, A.W., J.M. Smith, and J. Dubochet. 1986. Cryo-electron microscopy of vitrified chromosomes in situ. *EMBO (Eur. Mol. Biol. Organ.) J.* 5:1395–1402.

Melby, T.E., C.N. Ciampaglio, G. Briscoe, and H.P. Erickson. 1998. The symmetrical structure of SMC and MukB proteins: long, antiparallel coiled coil, folded at a flexible hinge. *J. Cell Biol.* 142:1595–1604.

Nicklas, R.B. 1983. Measurements of the force produced by the mitotic spindle in anaphase. *J. Cell Biol.* 97:542–548.

Oberhauser, A.F., P.E. Marszalek, H.P. Erickson, and J.M. Fernandez. 1998. The molecular elasticity of the extracellular matrix protein tenascin. *Nature.* 393:181–185.

Okada, T.A., and D.E. Comings. 1980. A search for protein cores in chromosomes: is the scaffold an artifact? *Am. J. Hum. Genet.* 32:814–832.

Ott, A., M. Magnasco, A. Simon, and A. Libchaber. 1993. Measurement of the persistence length of polymerized actin using fluorescence microscopy. *Phys. Rev. E.* 48:R1642–R1645.

Paulson, J.R., and U.K. Laemmli. 1977. The structure of histone-depleted metaphase chromosomes. *Cell.* 12:817–828.

Poljak, L., and E. Käs. 1995. Resolving the role of topo II in chromatin structure and function. *Trends Cell Biol.* 5:348–354.

Rattner, J.B. 1992. Integrating chromosome structure with function. *Chromosoma.* 101:259–264.

Rief, M., M. Gautel, F. Oesterhelt, J.M. Fernandez, and H.E. Gaub. 1997. Reversible unfolding of individual titin immunoglobulin domain. *Science.* 276: 1109–1112.

Saitoh, Y., and U.K. Laemmli. 1994. Metaphase chromosome structure: band arises from a differential folding path of the highly AT-rich scaffold. *Cell.* 76: 609–622.

Sedat, J., and L. Manuelidis. 1978. A direct approach to the structure of eukaryote chromosomes. *Cold Spring Harbor Symp. Quant. Biol.* 42:331–350.

Smythe, C., and J.W. Newport. 1991. Systems for the study of nuclear assembly, DNA replication, and nuclear breakdown in *Xenopus laevis* egg extracts. *Methods Cell Biol.* 35:449–468.

Strunnikov, A.V. 1998. SMC proteins and chromosome structure. *Trends Cell Biol.* 8:454–459.

Tskhovrebova, L., J. Trinik, J.A. Sleep, and R.M. Simmons. 1997. Elasticity and unfolding of single molecules of the giant muscle protein titin. *Nature.* 387: 308–312.